行政院國家科學委員會專題研究計畫　期中進度報告

利用化學控制合成新穎電子/離子作用氧化物及其特性分析

(2/3)

計畫類別：個別型計畫
計畫編號：NSC92-2113-M-002-036-
執行期間：92 年 08 月 01 日至 93 年 07 月 31 日
執行單位：國立臺灣大學化學系暨研究所

計畫主持人：劉如熹

計畫參與人員：王健源、張嵩駿、周大為、陳浩銘、林益山、黃妃婷、魏景怡、黃健博、彭歆傑

報告類型：精簡報告
報告附件：出席國際會議研究心得報告及發表論文
處理方式：本計畫可公開查詢

中　華　民　國 93 年 5 月 28 日

行政院國家科學委員會補助專題研究計畫成果報告

※※※※※※※※※※※※※※※※※※※※※※※※※

※　　　　　　　　　　　　　　　　　　　　　　　　※

※　利用化學控制合成新穎電子/離子作用氧化物　※

※　　　　　　及其特性分析(2/3)　　　　　　※

※※※※※※※※※※※※※※※※※※※※※※※※※

計畫類別：☑個別型計畫　　□整合型計畫

計畫編號：NSC 92-2113-M-002-036

執行期間：92 年　8 月　1 日 至 93 年　7　月　31 日

計畫主持人：劉如熹

本成果報告包括以下應繳交之附件：

□赴國外出差或研習心得報告一份

□赴大陸地區出差或研習心得報告一份

☑出席國際學術會議心得報告及發表之論文各一份

□國際合作研究計畫國外研究報告書一份

執行單位：台灣大學化學系

中　華　民　國　九 十 三 年　五　月 二 十 八 日

行政院國家科學委員會專題研究計畫成果報告
利用化學控制合成新穎電子/離子作用氧化物及其特性分析(2/3)
Synthesis by Chemical Control and Characterization of New Electronic/Ionic Oxides

計畫編號：NSC 92-2113-M-002-036
執行期限：92 年 8 月 1 日至 93 年 7 月 31 日

主持人：劉如熹 教授（台灣大學化學系）
計畫參與人員：王健源、張嵩駿、周大為、陳浩銘、林益山
黃妃婷、魏景怡、黃健博、彭歆傑
（台灣大學化學系）

一、中文摘要

自 1995 年具穿隧式磁電阻 (tunneling magnetoresistance; TMR)效應之材料得到突破性之進展，短短幾年內，其磁性感應度即提高一倍以上。TMR 於室溫時之 25~50 % 磁電阻值，遠遠高於傳統之巨磁電阻(giant magnetoresistance; GMR)材料(室溫~ 10 %)，使其對於各式紀錄媒體而言更具發展潛力。有鑑於此，本研究乃探討於 Sr_2CrMoO_6 ($Sr_2BB'O_6$)雙層鈣鈦礦化合物中，固定鹼土族鍶離子，藉由不同 3*d*、4*d* 與 5*d* 之過渡金屬離子，取代 B 或 B′之位置。計合成以 $3d^3$(Cr)為主之 Sr_2CrMoO_6 (Cr^{3+}：Mo^{5+} ⇔ $3d^3$：$4d^1$) 與 Sr_2CrWO_6 (Cr^{3+}：W^{5+} ⇔ $3d^3$：$5d^1$)系統，進而研究其晶體結構、磁性、電性等性質。藉由本研究之探討將可對化學取代效應，對於雙層鈣鈦礦化合物之穿隧磁電阻特性影響有完整之瞭解。希望藉由本研究之結果能促使更新之穿隧磁電阻材料被發現。

關鍵詞：穿隧式磁電阻、雙層鈣鈦礦、Sr_2CrMoO_6、Sr_2CrWO_6.

一、Abstract

Since 1995 materials of TMR (tunneling magnetoresistance) effect were improved evidently, in few years it's magnetic induction rose double. TMR materials show much higher MR% (about 25~50%) than traditional GMR materials (about 10%) under room temperature, so it is considered to apply MR sensor for the magnetic recording industry. Accordingly, in this research the Sr_2CrMoO_6 ($Sr_2BB'O_6$) double perovskites compounds were fabricated by keeping the stoichiometry of the alkaline earth strontium ion and substituting the position of B or B′ with different 3*d*, 4*d* and 5*d* transition metals. Therefore$CrFe^{3+}$：Mo^{5+} ⇔ $3d^3$：$4d^1$) and Sr_2CrWO_6 (Cr^{3+}：W^{3+} ⇔ $3d^3$：$5d^1$) systems have been synthesized. Moreover, their crystal structures, magnetic and electrical properties have been studied. The influences of the chemical replacement on double perovskites compounds with the TMR effect have been studied in this research. Based on this study it is hoped to arrive useful information on the exploration of new TMR materials.

Keywords: tunneling magnetoresistance (TMR)、double perovskites、Sr_2FeMoO_6、Sr_2FeWO_6

二、緣由與目的

Recently, Sr_2FeMoO_6 and Sr_2FeReO_6 have been known as prospective magnetoresistance compounds, which show an appreciable intrinsic tunneling-type magnetoesistance (TMR) at room temperature (RT) in the polycrystalline form [1-3]. These features are due to their half-metallic nature and a relatively high Curie temperature (T_C). In a simple picture, FeO_6 and MoO_6 octahedral alternate arrangement in the crystal structure of Sr_2FeMoO_6; the ferrimagnetic structure can be described as an ordered arrangement of parallel Fe^{3+} ($3d^5$, S = 5/2) magnetic moments, antiferromagnetically coupled with Mo^{5+} ($4d^1$, S = 1/2) spins. Thus a saturation magnetization of Ms = 4 μ_B is predicted. Indeed, the Ms values of bulk materials reported so far are systematically much smaller than the predicted 4 μ_B. This fact seems to be related to anti-site effects resulting from partial disorder of Fe and Mo ions among the B/B′ sublattices [4-7].

In relation to the electronic configurations of the Sr_2FeMoO_6, the average valence for Fe was also been found to be intermediate between high spin configurations values of Fe^{2+} and Fe^{3+} from Mössbauer spectroscopy studies [8-9]. This suggests that both electronic configurations with Fe^{2+} and Fe^{3+} must be considered as degenerate, with the final state being a combination of both configurations. On the other hand, tunneling-type magnetoresistance havs also been reported on Cr-based double perovskites A_2CrMO_6 (A = Sr, Ca; M = Mo, W, Re) compounds [10-12]. The major difference between Fe-based and Cr-based double perovskites oxides is that in the Cr

compound, there can be no valence degeneracy between the Cr and the Mo, W ions, since Cr can only be in the 3+ state ($3d^3$). Anyway, at this stage a very little research has been clarified on their physical measurements by X-ray absorption spectroscopy (XAS) and band structure calculations. In this study, we report the synthesis and characterization of the Sr_2CrMO_6 (M = Mo, W) samples with a particular focus on the effect of the variation of B′-site transition metal on the physical properties. The measured O (oxygen) K-edge X-ray absorption is in agreement with the calculated O *p*-density of states for both the compounds

三、研究方法

Sample Preparation. The samples of Sr_2CrMO_6 (M = Mo, W) were prepared by solid state reaction. The stoichiometric mixtures of high purity oxides $SrCO_3$, Cr_2O_3 or MoO_3 and WO_3 were calcined at 800 °C for 12 h in air. The obtained powders were ground and pressed into pellets. The pellets of Sr_2CrMoO_6 were then sintered at 1500 °C for 10 h in 5 % H_2 / N_2 gas mixture. However, the pellets of Sr_2CrWO_6 were sintered at 1550 °C for 12 h in 5 % H_2 / N_2 gas mixture.

Characterization. X-ray diffraction (XRD) measurements were carried out on a SCINTAG (X1) diffractmeter (Cu Kα radiation, λ = 1.5406 Å) at 40 kV and 30 mA. The GSAS program [13] was used for the Rietveld refinements in order to obtain information on the crystal structures of Sr_2CrMO_6 (M = Mo, W). Electron diffraction (ED) and high resolution transmission electron microscopic(HRTEM) study were carried out using a JEOL 4000EX electron microscope operated at 400 kV. Image simulation was made using CaRIne software. The resistively measurements were performed with a Quantum Design PPMS, using the conventional four-probe technique. Magnetization measurements were performed on a SQUID magnetometer from 0 to 350 K. The Cr K-edge X-ray absorption near edge structure (XANES) measurements was performed in transmission mode at the S-5B/W20 X-ray Wiggler beamline. The O K-edge XANES measurements were performed at a 6-m high-energy spherical grating monochromator (HSGM) beamline. Band structures of cubic Sr_2CrMO_6 (M = Mo, W) were calculated using the all-electron full-potential theory linear augmented plane wave (FLAPW) method [14]. The calculations were based on first-principles density functional theory (DFT) with the generalized gradient approximation (GGA) to the exchange-correlation potential.

三、結果與討論

The Fig. 1 (a) and (b) display the observed and calculated XRD patterms at 300 K for Sr_2CrMO_6 (M = Mo, W) samples. All the observed peaks can be fitted with the reflection conditions of the space group *Fm3m* for Sr_2CrMO_6 (M = Mo, W). The possibility of anti-site disordering due to some Mo or W sites being occupied by Cr atoms and vice versa was taken into account. The refined occupancies of the Cr and Mo(W) sites shows that the ratios of Cr/Mo and Cr/W anti-site disorder are around 43 % and 19%, respectively. Sánchez et al [15]. proposed that the actual degree of order depends mainly on synthesis conditions. Therefore, an increase in order in Sr_2CrWO_6 may be obtained by increasing the synthesis temperature.

Fig. 2 (a) and 2 (b) show a typical ED pattern and HRTEM lattice image, recorded along the [110] zone-axis direction of Sr_2CrWO_6. The simulated pattern along zone axis [110] is shown in Fig. 2 (c). The lattice image is belonging to a cubic cell with a = b = c = 7.8 Å .The cell symmetry obtained by ED was identified by the observation only of *h k l* reflections indicating *F*-centering of the unit cell which is consistent with the XRD refinement result.

The plot magnetic susceptibility (χ) vs. temperature (T) (as shown in Fig. 3) indicates that (a) Sr_2CrMoO_6 and (b) Sr_2CrWO_6 is an antiferromagnet with T_N = 40 K and 30 K at H = 1 T, respectively. As shown in Fig. 3 (a) and (b), the Curie-Weiss plot for Sr_2CrMO_6 (M = Mo, W) reasonably well for T＞150 K give positive Weiss temperature θ ~ 83 K and 18 K at H = 1 T, respectively. These data suggest that although there exists both ferro- and antiferromagnetic interactions, the ferromagnetic interaction dominates over the antiferromagnetic one.

The transport properties of Sr_2CrMO_6 (M = Mo, W) samples are illustrated in Fig. 4. Both ρ(H = 0 T) and ρ(H = 3 T) show a semiconductor-like behavior over the whole temperature range up to 5 K. The resistivities (ρ) of Sr_2CrWO_6 sample (about 10^3 Ω cm) is higher than Sr_2CrMoO_6 (about 10^2 Ω cm). The plots of magnetoresistance (MR) against temperature for Sr_2CrMO_6 (M = Mo, W) are also given in the inset of Fig. 4. The MR ratio is define as MR (T,H) = [ρ (T,H = 0) - ρ (T,H = 3 T)]/ ρ (T,H = 3 T)] where H denotes the external field. The large magnetoresistance ratio (MR) of ~38 % (H = 3 T) at 5 K was observed in the Sr_2CrWO_6 compound. However, the Sr_2CrMoO_6 compound did not show any significant MR even at high fields (MR ~ 4 %; H = 3 T and 5 K).

In Fig. 5 (a) we show the Cr K-edge XANES spectrum of Sr_2CrMO_6 (M = Mo, W), the spectra of Cr^{3+} in standard Cr_2O_3, and the Cr^{4+} in standard CrO_2 are also plotted. In Fig. 5 (a) Pre-edge features of A and B result from transitions to bound the final states in the 3*d* orbital. Moreover, there is a relatively intense and symmetric resonance above the absorption edge (C), and a broader structure to high energy (D). The rising part of the Sr_2CrMO_6 (M = Mo, W) main edge can be seen to have a chemical shift identical to that of the Cr^{3+} standard and well separated from that of the Cr^{4+} standard. To obtain detailed information on the electronic and geometric

structures around the Cr ion, the pre-edge features of the Cr K-edge XANES spectrum is show in the Fig. 5 (b). Moreover, the Sr_2CrMO_6 (M = Mo, W) pre-edge manifests a three-features (k1, k2 and k3) structures, similar to the Cr^{3+} standard , whereas the Cr^{4+} standard has a were separated bimodal-feature structure. Among the Cr^{4+} materials the sharp low energy k1-feature is particularly distinctive with the intensities and positions of the k2 and k3 features which is varying between compounds. Therefore the structure of the pre-edge further supports the assignment of a Cr^{3+} state in Sr_2CrMO_6 (M = Mo, W).

We also performed X-ray absorption spectroscopic (XAS) measurements at O K-edge. The spectra were recorded by measuring the X-ray fluorescence yield technique at room temperature. The experimental XAS spectra are displayed in Fig. 6 together with the calculated O p-DOS spectra. Clearly, there is a good agreement between XAS and O p-DOS over the whole energy range studied, indicating that the present theoretical description of the electronic structure for the Cr-based double perovskites is rather adequate.

五、結論

In order to investigated the interaction among 3*d*(Cr), 4*d*(Mo) and 5*d*(W) orbitals of transition metal ions via oxygen ions, the crystal structure, magnetic and magnetotransport properties of B´-site transition metal Sr_2CrMO_6 (M = Mo, W) with double perovskites structure have been systematically investigated. The powder XRD analyse revealed that Sr_2CrMoO_6 and Sr_2CrWO_6 have a cubic cell (space group: *Fm3m*). The Curie-Weiss plot for Sr_2CrMO_6 (M = Mo, W) reasonably well for T＞150 K give positive Weiss temperature θ ~ 83 K and 18 K at H = 1 T, respectively. These data suggest that although there exists both ferro- and antiferromagnetic interactions, the ferromagnetic interaction dominates over the antiferromagnetic interaction. This behavior is in good agreement with the band structure calculations data.

六、計畫成果自評

We have reached the goals of the research plan, some part of the results have already publicized in scientific journals [15-19].

七、參考文獻

[1] K.-I. Kobayashi, T. Kimura, H. Sawada, K. Terakura, Y. Tokura, Nature 395 (1998) 677.

[2] K.-I. Kobayashi, T. Kimura, H. Sawada, K. Terakura, Y. Tokura, Phys. Rev. B 59 (1999) 11159.

[3] T.H. Kim, M. Uehara, S.W. Cheong, S. Lee, Appl. Phys. Lett. 74 (1999) 1737.

[4] G. Prince, Science 282 (1998) 1660.

[5] Y. Tomioka, T. Okuda, Y. Okimoto, R. Kumai, K.-I. Kobayashi, Y. Tokura, Phys. Rev. B 61 (2000) 422.

[6] R.P. Borges, R.M.Thomas, C. Cullinan, J.M.D. Coey, R. Suryanarayan, L. Ben-Dor, L. Pinsard-Gaudart, A. Revcolevschi, J. Phys.: Condens. Matter 11 (1999) L445.

[7] L. Balcells, J. Navarro, M. Bibes, A. Roig, B. Martinez, J. Fontcuberta, Appl. Phys. Lett. 78 (2001) 781.

[8] P.M. Woodward, Acta Crystallogr Sect. B 53 (1997) 32.

[9] M.C.Viola, M.J. Martínze-Lope, J.A. Alonso, P. Velasco, J.L. Martínze, J.C. Pedregosa, R.E. Carbonio, M.T. Fernández-Díaz, Chem. Mater. 14 (2002) 812.

[10] A. Arulraj, K. Ramesha, J. Gopalakrishnan, C.N.R. Rao, J. Solid State Chem. 155 (2000) 233.

[11] J.B. Philipp, D. Reisinger, M. Schonecke, A. Marx, A. Erb, L. Alff, R. Gross, Appl. Phys. Lett. 79 (2001) 3654.

[12] H. Kato, T. Okuda, Y. Okimoto, Y. Tomioka, Appl. Phys. Lett. 81 (2002) 328. 2003, **15**, 425.

[13] A.C. Larson, R.B.Von Dreele, Generalized Structure Analysis System (GSAS), Los Alamos National Laborator Report LAUR, 1994 86-748.

[14] P. Blaha, K. Schwarz, G.K.H. Madsen, D. Kvasnicka, J. Luitz, WIEN2k, An Augmented Plane Wave + Local Orbitals Program for Calculating Crystal Properties (Karlheinz Schwarz, Techn. Universitat Wien, Austria), 2001 ISBN 3-9501031-2 .

[14] D. Sánchez, J.A. Alonso, M. García-Hernández, M.J. Martínze-Lope, J.L. Martínez, Phys. Rev. B 65 (2002) 104426.

[15] S.F. Hu, R.L. Yeh, R.S. Liu, J. Vac. Sci. Tech. B 22 (2004) 60.

[16] R.S. Liu, S.C. Chang, J.M. Chen, Chin. J. Phys., in press.

[17] S.W. Lin, S.C. Chang, R.S. Liu, S.F. Hu, N.T. Jan, J. Mag. Mag. Mat., in press.

[18] R.S. Liu, S.C. Chang, J.M. Chen, Super. Sci. Technol., in press.

[19] T.S. Chan, R.S Liu, G.Y. Guo, S.F. Hu, J.G. Lin, J.M. Chen, C.-R. Chang, Submitted to Solid. State Comm.

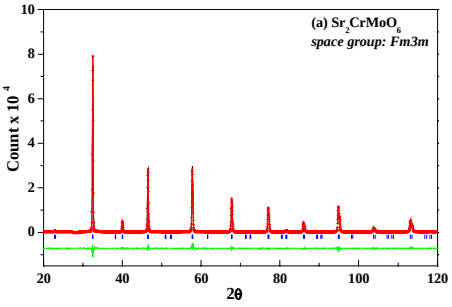

Fig 1. Rietveld fits for powder XRD data of Sr_2CrMO_6 (M = Mo, W) with (a) Sr_2CrMoO_6 and (b) Sr_2CrWO_6 space group *Fm3m*, at 300K. Observed (crosses) and calculated (solid line) intensities are shown with the difference at the bottom.

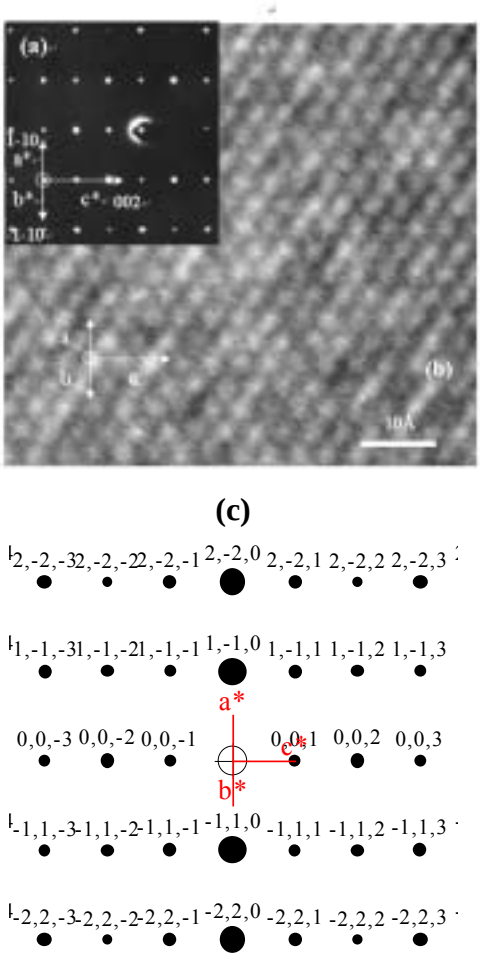

Fig 2. (a) ED pattern and (b) HRTEM lattice image along the [110] direction of Sr_2CrWO_6 sample. (c) Simulated pattern along the zone axis [110].

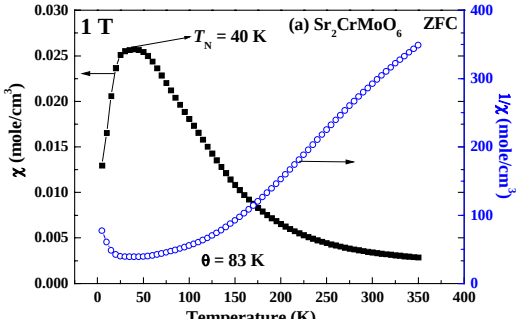

Fig 3. Temperature dependence of Magnetic susceptibility (χ) and Curie-Weiss plot for (a) Sr_2CrMoO_6 and (b) Sr_2CrWO_6 in the temperature from 5 K to 350 K.

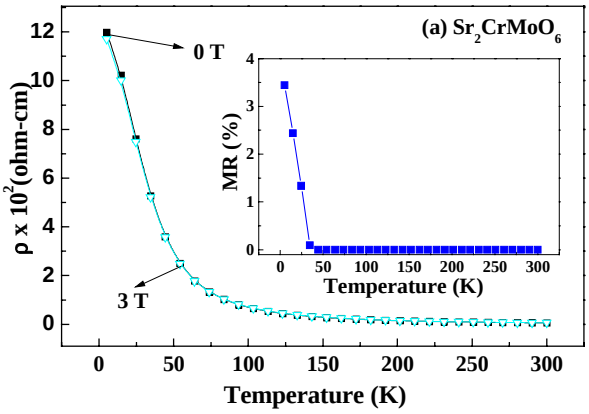

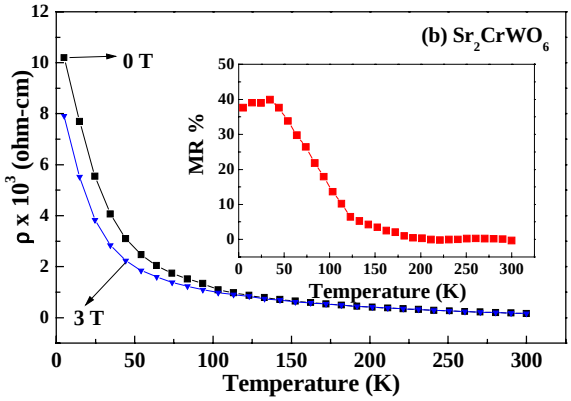

Fig 4. Temperature dependence of resistivity at a magnetic field of 0 T and 3 T of Sr_2CrMO_6 (M = Mo, W) with (a) Sr_2CrMoO_6 and (b) Sr_2CrWO_6. (b) Plot of MR% against temperature of Sr_2CrMO_6 (M = Mo, W) is also given in the inset.

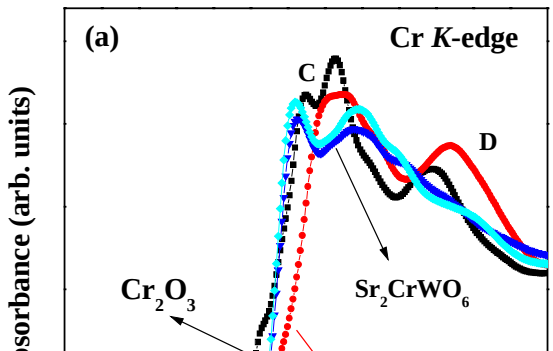

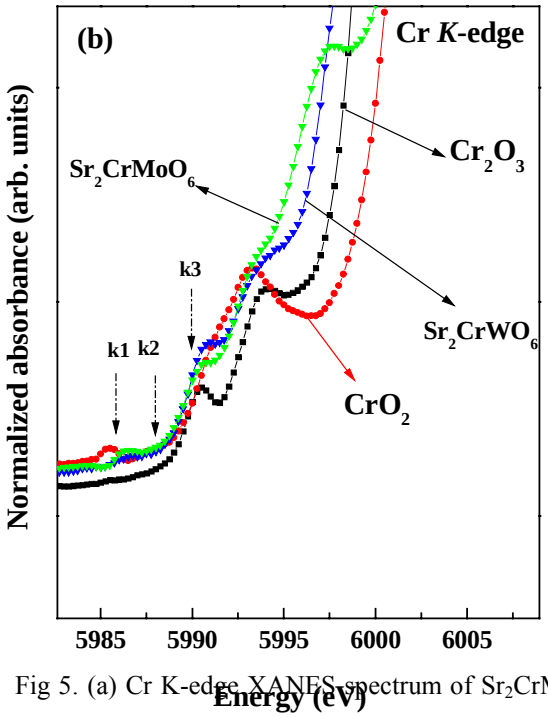

Fig 5. (a) Cr K-edge XANES spectrum of Sr_2CrMO_6 (M = Mo, W), the spectra of Cr^{3+} in the standard Cr_2O_3, and the Cr^{4+} in the standard CrO_2 are plotted. (b) Cr K-edge XANES pre-edge spectra of Sr_2CrMO_6 (M = Mo, W) with manifests a three-features (k1, k2 and k3) structures.

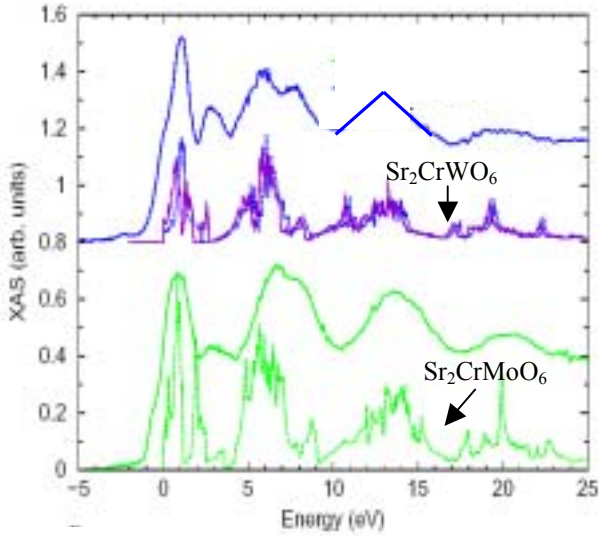

Fig 6. O *K*-edge X-ray absorption spectrum (XAS) and O *p*-decomposed DOS of Sr_2CrMO_6 (M = Mo, W).